GLASIUS BIO-INSPIRED NEURAL NETWORK ALGORITHM-BASED SUBSTATION INSPECTION ROBOT DYNAMIC PATH PLANNING

Wei Zhang,* Xiaoliang Feng,** and Bing Sun***

Abstract

This study presents a glasius bio-inspired neural network (GBNN) algorithm for intelligent substation inspection robot autonomous path planning. First, a GBNN Neural map is established to represent the working environment of the inspection robot. In this model, each neuron corresponds to a grid map position unit. The GBNN model was trained to map the environment, including obstacles and potential paths, into a discrete neural network representation. Second, the motion path of the inspection robot was planned autonomously based on the activation output values of the neurons in the neural network. The robot selected the path with the highest activation output value for the next movement direction. The simulation results under dynamic obstacle scenarios or in uncertain environments demonstrated the effectiveness of the GBNN algorithm in path planning.

Key Words

Substation inspection robot, path planning, glasius bio-inspired neural network, dynamic obstacle

1. Introduction

Intelligent substations are one of the most important parts of a smart grid and are exposed to long-term safety hazards in the field. To prevent grid accidents, substations must be inspected and maintained regularly. Traditional manual inspection, which is labour-intensive [1], is inefficient and may be dangerous, particularly in thunderstorms and other adverse weather conditions. There is a significant safety risk and it cannot be promptly inspected. Recently, intelligent inspection robots have gradually replaced manual inspection. Intelligent inspection robots are equipped with various sensors and measuring devices to independently perform electrical equipment inspection tasks [2]. These robots use thermal infrared imaging sensors to monitor oil levels and temperatures, Pan-Tilt-Zoomcameras [3] to monitor breaker situations, partial-discharge detection devices to track lightning arrester actions, and other measuring devices to detect internal thermal and external machinery defects.

This study focuses on path planning for inspecting robots, which refers to determining an available path from the starting position to the target point while avoiding obstacles in the workspace. Common methods include artificial potential field (APF) [4]–[6], grid method [7], A* algorithm [8], [9], particles warm optimisation method [10], other heuristic approach method [7], and even complete path coverage methods such as the Glasius bio-inspired neural network (GBNN) [11] and Voronoi partition-based coverage [12]–[14]. However, these methods have shortcomings when applied under different working conditions. For example, the grid method is limited by sensors and requires excessive computational resources. The A* algorithm often results in paths with many turns, large cumulative turning angles, and the stander A* method always not consider dynamic obstacles [8], [9]. The APF method may have local extremum points and oscillate in narrow passages. In [15], a learning-free and adaptive bio-inspired neural network algorithm called the GBNN was proposed and applied to full-coverage path planning for mobile robots.

In the GBNN algorithm, the neurons in the bio-inspired neural network correspond one-to-one to the cells in a 2D grid map of the target area, and the external inputs of the neurons are determined based on the status of the cells in the grid map. Thus, the activation values of the neuron scan be calculated

* Department of Electrical Engineering, Shanghai Dianji University, Shuihua Road 300, Shanghai 201306, China; e-mail: viweizhang@163.com

** Department of Electrical Engineering, Shanghai Dianji University, China, Shuihua Road 300, Shanghai 201306, China; e-mail: fengxl2002@163.com

*** Department of Logistic Engineering Colleague, Shanghai Maritime University, Haigang Avenue 1550, Shanghai 201306, China; e-mail: hmsunbing@163.com

Corresponding author: Wei Zhang

Recommended by Hao Zhang
(DOI: 10.2316/J.2024.206-1046)

directly, and the path of the robot can be determined by the activation values of the neural network and its previous path. This algorithm does not require any neural network learning or training processes and exhibits good real-time performance. Furthermore, the GBNN method has been widely applied in various fields, including complete coverage path planning for autonomous underwater vehicles (AUV) [16] and mobile robot [17], [18], cooperative path planning for unmanned surface vehicles (USV) [19], [20], multi-robot distributed collaborative region coverage search [15], energy efficiency for complete coverage path planning of ship hull maintenance [21], and the substation inspection path planning [22], [23]. In [16], the GBNN method was introduced for single AUV complete coverage and combined with the centroidal Voronoi tesselation distribution method for multi-AUV complete coverage path planning. In [17], the GBNN method was combined with a backtracking algorithm to reduce the path repetition ratio for complete coverage path planning of mobile robots. In [18], GBNN-based UV-C disinfection path planning was improved by using a preventive deadlock-processing algorithm. In [20], the GBNN algorithm was used for USV path planning for multi-USVs, and the Hungarian algorithm was built and modified for task assignment. In [23], considering the constraints for a multi-robot system to perform a region coverage search task in an unknown environment, a novel multi-robot distributed collaborative region coverage search algorithm based on a GBNN was developed, and the simulation results showed good performance.

The path planning of inspection robots has been conducted by scholars; However, further research is required. In [24], the robot system for substation equipment inspection consisted of a wheeled mobile robot and data center. The mobile robot could park at designated stop points and rotate its platform to obtain images and temperature information. However, a drawback is that multiple landmarks must be laid out beforehand in the substation to guide the navigation of the robot. In [22], an optimisation algorithm for power system inspection that minimises the number of inspection teams and the length of inspection paths was proposed by combining an improved k-means algorithm and an ant colony algorithm. In [23], a bio-inspired neural network method (BINN) has been proposed to study the multi-robot substation inspection problem, based on this method can effectively reduce the path length and number of turns during special inspections and routine inspections, but not consider the dynamic obstacles. Considering the characteristics of power substations and the potential encounter of dynamic obstacles during the inspection process, this study focuses on dynamic path-planning methods for inspecting robots based on the GBNN algorithm. Specifically, we built on the basic GBNN model and extended it to incorporate the dynamics of the environment.

At present, there are few studies on substation inspection robot path planning, and the influence of dynamic obstacles in the inspection process and the path planning problem under emergency working conditions are not considered. The remainder of this paper is organised as follows. Section 2 describes the GBNN based substation inspection robot-path planning. Then, the GBNN algorithm-based dynamic path planning for a substation inspection robot with dynamic obstacles considering congested road sections and even urgent tasks during the inspection process is presented in Section 3. Finally, concluding remarks are presented in Section 4.

Figure 1. Inspection robot inspecting illustration.

2. Substation Inspection Robot Path Planning

The basic principle of the GBNN algorithm-based substation inspection robot path planning is to establish a bio-inspired neural network model based on a substation grid map. The GBNN model was used to represent the working environment of the inspection robot, and a one-to-one correspondence was established between the neural network and the substation grid map. Based on the activation output value distribution of the neurons in the neural network, the inspection robot autonomously planned a collision-free inspection path.

2.1 Mapping of Substation Environment

An operational schematic of the intelligent substation inspection robot is shown in Fig. 1. During the inspection process, the robot utilises various sensors, such as cameras and radar, in addition to substation environment information to perceive obstacles. An inspection robot can combine this information and transform it into binary-image information. Based on the substation environment map, the GBNN algorithm is applied to the inspection robot path plan. To achieve real-time reflection of environmental changes in the neural network activity value, the neural network must be closely integrated with the substation environment. Environmental information is typically continuous, while neural networks are discrete. Therefore, it is necessary to discretise the substation environment and create a grid map [23], as shown in Fig. 2.

In research on intelligent substation inspection robot path planning, we consider the inspection robot as a point mass and ignore its motion model. Owing to the grid resolution and actual area of the intelligent substation environment, the number of grid units in the substation is determined. In this study, we consider a 220 kV substation as an example, and the actual 5 m $\times$ 5 m units are gridded into 1 $\times$ 1 grid units, as shown in Fig. 2. The black grids in Fig. 2 represent the buildings and electrical equipment in the intelligent substation, including, the control room,

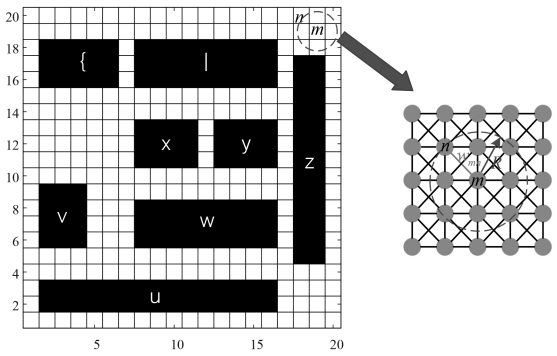

Figure 2. The substation path planning environment map and GBNN neural map: (a) the substation path planning environment map; (b) the neural map corresponding to the environment map.

main transformer, high-voltage room, capacitor equipment area, 10 kV transformer, and 220 kV equipment area. As shown in Fig. 2(a), these static obstacles mainly include the following areas: u is the power capacitor equipment zone, v is the main control building, w is the 10 kV high voltage equipment, x is the No.1 main transformer, v is the No.2 main transformer, z is the 110 kV equipment area, and { and | are 220 kV equipment areas.

2.2 GBNN Algorithm

The GBNN is an improved BINN inspired by the performance of Hopfield neural networks [16]. The GBNN method, which utilises differential equations, offers numerous advantages for learning and adaptation. This approach not only reduces the calculation load but also enhances the operational speed of the algorithm, resulting in a more effective path planning solution for substation robots. Each neuron in the network is characterised by a shunting equation derived from Hodgkin and Huxley's membrane model for biological neural systems, leading only to local lateral connections among neurons. The dynamic behavior of a neural network is described by the following equation:

$$\frac{du_k}{\mathrm{dt}} = -Au_k + (B - u_k)\left([I_k]^+ + \sum_{i=1}^{M} w_{\mathrm{kl}}\,[u_l]^+\right) - (D + u_k)\,[I_k]^- \tag{1}$$

where u_k is the neural activity of k th neuron, u_l is the active value of its adjacent neurons l, M is the neuron number adjacent to neuron k, I_k is the external input of neuron k and it can be represented as (2), $[I_k]^+ = \max[I_k, 0]$ represents an external excitatory signals, $[I_k]^- = \max[-I_k, 0]$ represents external inhibitory signal, and w_{kl} is the connection weight between the kth neuron and lth neuron.

$$I_k = \begin{cases} E, & \text{Target} \\ -E, & \text{Obstacle} \\ 0, & \text{Others} \end{cases} \tag{2}$$

The GBNN algorithm is a discrete-time Hopfield-type neural network, as illustrated in Fig. 2(b). Each circle in the figure represents a neuron with activity values that can be transmitted through connections. The dynamic behaviour of individual neuron activities is described by the following law:

$$x_i(t+1) = g\left(\sum_{j=1}^{M} w_{\mathrm{ij}}\,[x_j(t)]^+ + I_i\right) \tag{3}$$

where the transfer function is chosen as:

$$g(x) = \begin{cases} -1, & x < 0 \\ \beta \mathrm{x}, & 0 \le x < 1, \beta > 0 \\ 1, & x \ge 1 \end{cases} \tag{4}$$

In (2), $x_i(t+1)$ represents the activity of the ith neuron at time t+1, $x_j(t)$ represents the activity of the jth neuron at time t. The jth neuron is laterally connected to the ith neuron. $[x_j(t)]^+ = \max[x_j(t), 0]$ indicates that only positive neural activities can have a global impact on other neurons, whereas negative activities are limited to local effects and cannot propagate outward. I_i is the external input to the ith neuron. M is the number of connections between the ith neuron and its neighbouring neurons within the receptive field R. The connection weight between the ith neuron and jth neuron is represented by w_{ij} and is defined as follows:

$$w_{\mathrm{ij}} = \begin{cases} e^{-\alpha|i-j|^2}, & 0 < |i-j| \le R \\ 0, & |i-j| > R \end{cases} \tag{5}$$

where $|i-j|$ represents the Euclidean distance between ith neuron and jth neuron and α and R are positive constants.

To minimise energy consumption, planning the shortest path with minimal turns for substation inspection robots is crucial. Thus, the previous movement direction of the inspection robot must be considered in path planning. For the current location of inspection robot P_c, the next location P_n can be defined as follows [26]:

$$P_n \Leftarrow xP_n = \max\{x_k + cy_k, k = 1, 2, \ldots, m\} \tag{6}$$

The equation represents the neural activity x_k of the kth neuron, where c is a non-negative constant, m is the number of neighboring neurons at the current location P_c, and y_k is a monotonically increasing function that depends on the included angle φ_k between the current and next sailing directions of the inspection robot. The expression for y_k is given by

$$y_k = 1 - \frac{\Delta\varphi_k}{\pi} = 1 - \frac{|\varphi_k - \varphi_c|}{\pi} \tag{7}$$

where $\varphi_k = a\tan 2(y_{P_k} - y_{P_c}, x_{P_k} - x_{P_c})$, $\varphi_c = a\tan 2(y_{P_c} - y_{P_p}, x_{P_c} - x_{P_p})$. $P_p(x_{P_p}, y_{P_p})$, $P_c(x_{P_c}, y_{P_c})$, and $P_k(x_{P_k}, y_{P_k})$ represent the previous, current, and subsequent step positions, respectively, as shown in Fig. 3.

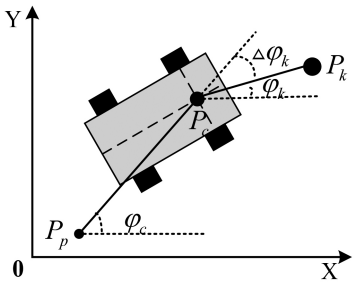

Figure 3. Movement direction of inspect robot.

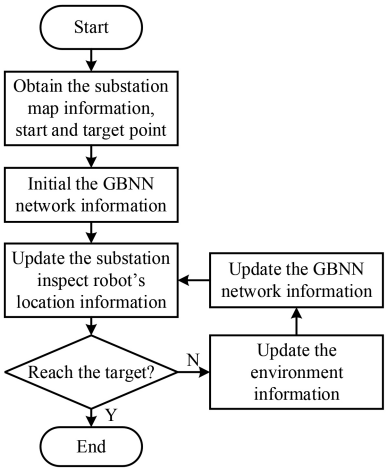

Figure 4. Flow chart of inspect robot path planning based on GBNN algorithm.

2.3 GBNNBased Inspect Robot Path Planning

The basic idea of the substation inspection robot path planning algorithm based on the GBNN proposed in this paper can be summarizsed as follows: establishing the substation grid map and a GBNN model, and a correspondence between the bio-inspired neural network and the map is established. Based on the activation values of the neurons in the substation grid map, the motion path of the inspection robot was planned to achieve collision-free path planning in a dynamic substation environment. The implementation process of substation inspection robot path planning based on the GBNN algorithm is shown in Fig. 4.

As shown in Fig. 4, the process for inspecting robot path planning based on the GBNN algorithm mainly includes the following steps: (1) obtaining the substation map information that includes the start and target point information, (2) initialising theGBNN network information, (3) updating the substation inspection robot's location information, (4) updating the environment information, and (5) updating the GBNN network information. Steps (3), (4), and (5) were repeated until the substation inspection robot reached its target. The substation inspection robot position was updated using (6). The GBNN network is updated by resetting it to zero and recalculating it. If a task is completed, then, the corresponding GBNN isreset to zero. Otherwise, the GBNN was recalculated.

3. Simulation and Discussion

In this section, we utilise MATLAB to perform the simulation experiment and represent the substation working environment using grid maps. In the simulation, we modelled all inspection robots as particles and set the parameters of the GBNN algorithm as follows [26]: $A = 10$, $B = D = 1$, $E = 100$, $\beta = 0{:}6$, $\alpha = 2$, $R = \sqrt{2}$, and $c = 0.5$. In the following, we compare different path planning methods and the GBNN-based inspection robot path plan effectiveness under normal conditions, considering dynamic obstacles, and under uncertain environments.

3.1 Comparison of Different Path Planning Methods

To assess the feasibility of GBNN path planning methods, we conducted a point-to-point path planning simulation. The simulation environment consists of electrical equipment and buildings marked with black grids, while the free space allows the inspection robot to navigate. The starting point is denoted by a red triangle, and the target point is represented by a red pentagram. Specifically, in Fig. 5(a), the starting point is set at point (4, 10), and the target is located at point (19, 4). Additionally, in Fig. 5(b), the target point (20, 16). To compare the performance of GBNN with other path planning methods, we employed three widely-used methods: A* algorithm and APF algorithm, as shown in Fig. 5. Upon analysing the simulation results in Fig. 5(a), we observed that the paths generated by GBNN, A*, and APF all successfully reached the destination. However, when we changed the target point, the APF algorithm, using the same parameters as in Fig. 5(a), exhibited poor generalisation properties. It was unable to plan a path that navigates through obstacles, as depicted in Fig. 5(b). Due to the A* method's primary application for static path planning without considering dynamic obstacles, we decided to focus on studying the performance of GBNN-based path planning under normal working conditions, considering dynamic obstacles and uncertain conditions for the subsequent parts of this study.

3.2 Normal Path Planning

To validate the effectiveness of the proposed algorithm, simulation analyses were conducted to evaluate the path planning performance of inspection robots in power substations performing point-to-point inspection tasks, based on the GBNN algorithm.

As depicted in Fig. 6, the inspection robot started from the main control building and performed a point-to-point inspection task. The starting points of the inspection robot is (4,10), indicated by the red triangle in Fig. 6(a), and the task point is (20,17), indicated by the red pentagon in Fig. 6(a). Figure 6(a) presents the inspection robot's planned path based on the GBNN algorithm, and Fig. 6(b) illustrates the GBNN neuron activity values under this

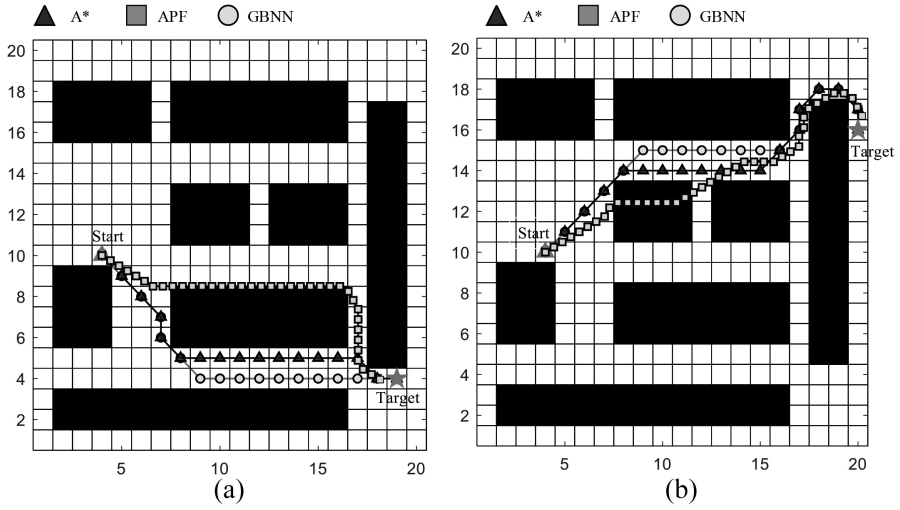

Figure 5. Comparison of different path planning methods.

Table 1
The Neighborhood Activity Value of the Start Point (4,10) Under Normal Path Planning

Position	Neural activity
(3,11)	9.1324E-29
(4,11)	9.2701E-28
(5,11)	7.7853E-27
(3,10)	1.2091E-29
(4,10)	1.0161E-28
(5,10)	6.8729E-28
(3,9)	−1.0000
(4,9)	−1.0000
(5,9)	6.3252E-29

condition. The neural network activity value of the task target point was 1, as shown in Fig. 6(b). Table 1 lists the activity values of starting point (4,10) and its eight adjacent neurons. As shown in Table 1, (3,9) and (4,9) represent obstacles with a neural network activity value of −1, and the neural network activity value of (5,11) corresponding to the point adjacent to the starting point (4,10) is the maximum value of the surrounding activity values, which is 7.7853E-27. Therefore, the inspection robot moved from starting point (4,10) to (5,11).

3.3 Path Planning Consider Dynamic Obstacle

To further analyse the GBNN algorithm-based path planning performance, we considered the dynamic obstacles appeared during inspection process. In the simulation, we considered that the obstacle appeared when the inspection robot reached the point (8,14) with partial or full coverage. The simulation results are shown in Fig. 7, and the neural activities around the obstacle are listed in Table 2.

Table 2
The Neighborhood Activity Value Around (9,15) under Static Obstacle

Position	Neural activity		
	Without obstacle on road	Partial coverage obstacle	Full coverage obstacle
(8,16)	−1.0000E+00	1.0000E+00	−1.0000E+00
(9,16)	−1.0000E+00	1.0000E+00	−1.0000E+00
(10,16)	−1.0000E+00	1.0000E+00	−1.0000E+00
(8,15)	1.3746E-20	9.7676E-22	6.5873E-25
(9,15)	2.6788E-19	−1.0000E+00	−1.0000E+00
(10,15)	5.2539E-18	5.2411E-18	6.2587E-26
(8,14)	1.0596E-20	8.5324E-21	2.0011E-24
(9,14)	1.9285E-19	1.7997E-19	−1.0000E+00
(10,14)	3.4669E-18	3.4648E-18	3.4563E-18

When a partial coverage obstacle appeared at the inspection point (9,15), the neural activation value changed from 2.6788E-19 to −1, as shown in Table 2, and when a full coverage obstacle appeared, the neural activation values of inspection points (9,15) and (9,14) both changed to −1. Figure 7 and Table 2 show that the obstacle appears before the inspection robot reaches the inspection point (9,15), causing the inspection robot to change its inspection path from the original path (8,14)→(9,15)→(10,15) to (8,14)→(9,19)→(10,15) with a partial coverage obstacle, and finally to (8,14)→(7,15)→(7,16) with a full coverage obstacle.

3.4 Path Planning for Uncertain Environments

During the operation of an intelligent substation inspection robot, obstacles, busy roads, or even urgent tasks

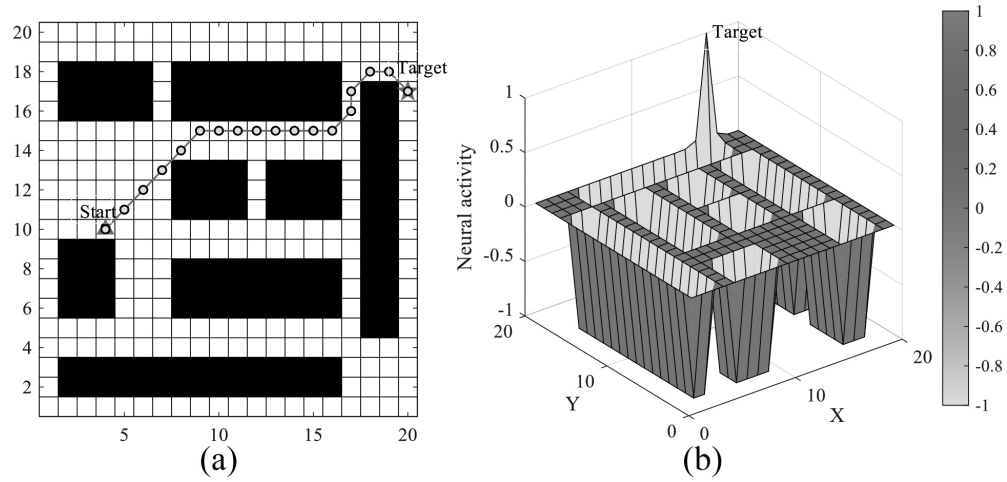

Figure 6. Point to point normal path planning: (a) path planning; (b) neural activity landscape.

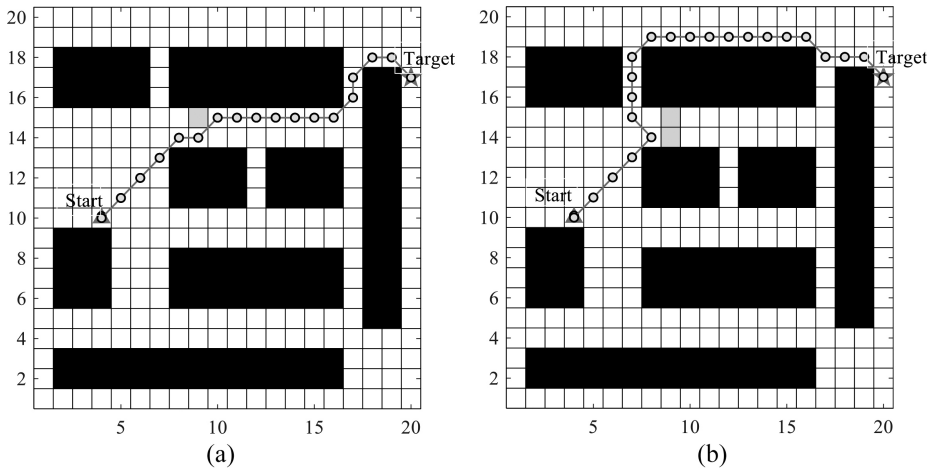

Figure 7. Path planning for the obstacle appeared during the inspection process: (a) partial coverage obstacle; (b) full coverage obstacle.

may be encountered, all of which pose challenges to the robot path planning. Based on these three uncertain working conditions, we analysed the corresponding inspection path of the robot using the GBNN method. The corresponding simulation results are shown in Fig. 8, and Table 3 lists the neighborhood activity values around (7,14) under an uncertain environment.

As shown in Fig. 8(a), during the inspection process of the robot from the starting point (3,5) to the target point (10,19), dynamic obstacle A, as indicated by the yellow grid, appears when the robot inspects point (4,5), and obstacle B appears when inspecting point (7,12). The inspection path of the robot was determined based on the GBNN algorithm. Comparing it with the inspection path without obstacles shown in Fig. 8(b), it can be seen that after the appearance of obstacle A, the inspection path of the robot changed from (4,5)→(5,6)→(6,7)→(7,8) to (4,5) →(5,5) →(6,5) →(7,6), and after the appearance of obstacle B, the inspection path of the robot changed from (7,12)→(7,13)→(7,14)→(7,15) to (7,12)→(6,13)→(5,14)→(4,15). Considering the busy road sections that may appear during the robot inspection process, as shown by the blue shadow in Fig. 8(c), the inspection path of the robot changed from (7,14)→(7,15) without considering congested road sections to (7,14)→(6,14).

Comparing the GBNN neuron activation values for the adjacent grid (7,14) before and after the appearance of busy road sections in Table 3, it can be observed that the neuron activation values for other grids remained unchanged because the inspection starting point and target point did not change. Figure 8(d) depicts a simulated study of the inspection path when congested road sections are considered, where the robot receives an urgent inspection task to go to the inspection location (12,15) while running at (3,14). Because the inspection target point of the robot changed, the neuron activation values for each grid changed accordingly (as shown in Table 3). The inspection path of the robot changed from (3,14)→(2,14)→(1,15)→(1,16)→(1,17)→(1,18), without an urgent task, to (3,14)→(4,14)→(5,14)→(6,14)→(7,15) →(8,15), until the new inspection goal point was reached.

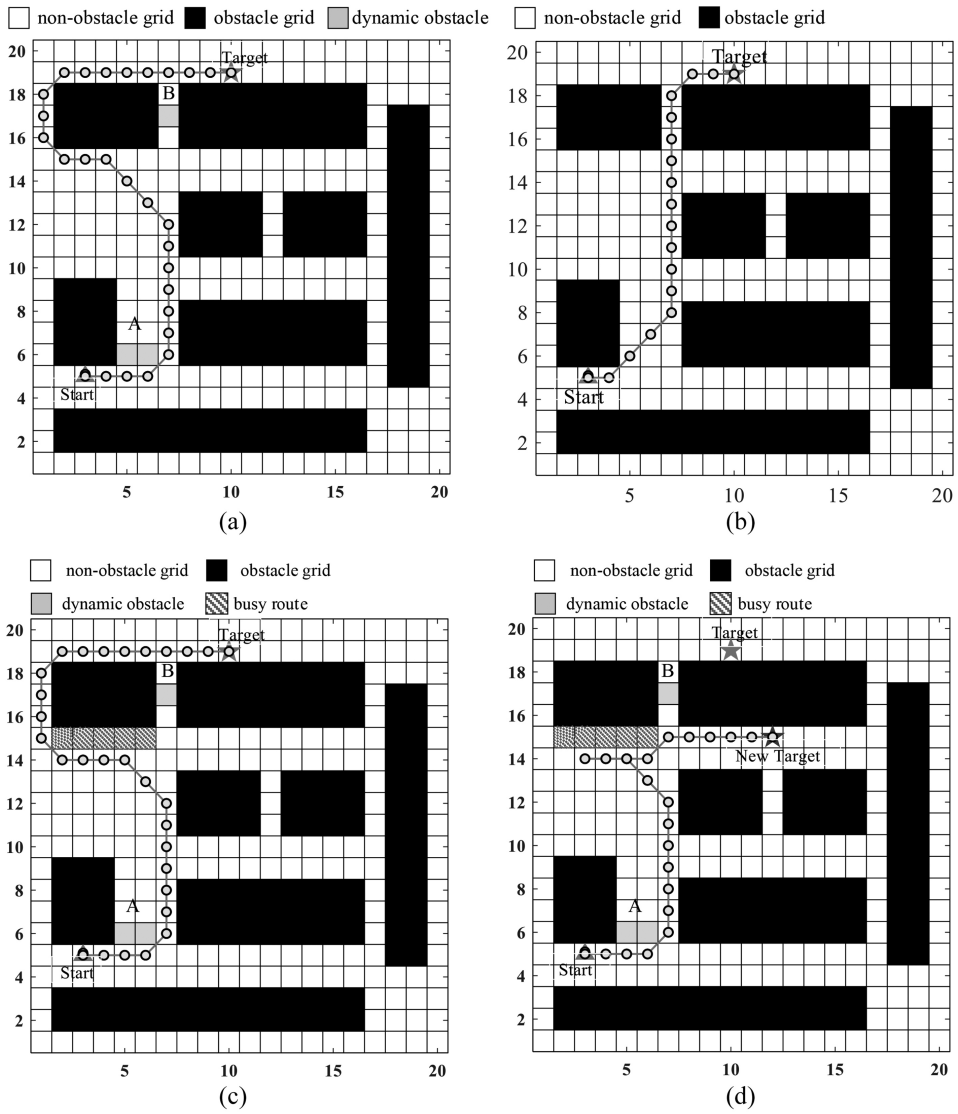

Figure 8. Path planning for the obstacle appeared during the inspection process: (a) path planning with dynamic obstacle; (b) path planning without obstacle.

Table 3
The Neighborhood Activity Value Around (7,14) under Uncertain Environment

Position	Neural activity			
	without obstacle on road	Dynamic obstacle	Obstacle with busy route	Obstacle with urgent task
(6,15)	1.5315E-10	1.4170E-23	−1.0000E-07	−1.0000E-07
(7,15)	1.3399E-09	7.1853E-25	7.1853E-25	2.7931E-07
(8,15)	1.5315E-10	7.2662E-26	7.2662E-26	5.5620E-06
(6,14)	1.4680E-11	7.4810E-24	7.4810E-24	8.9725E-09
(7,14)	6.5536E-11	4.4625E-25	4.4625E-25	1.5448E-07
(8,14)	1.4629E-11	5.3184E-26	5.3184E-26	2.6051E-06
(6,13)	1.0667E-12	2.0011E-24	2.0011E-24	1.6647E-09
(7,13)	3.2336E-12	1.4154E-25	1.4154E-25	1.5646E-08

4. Conclusion

The GBNN model was used in this study to investigate the autonomous path planning and safe obstacle avoidance of inspection robots based on a two-dimensional grid map of the substation. From the different path-planning comparisons between the A*, APF, and GBNN methods. The GBNN algorithm has a simple structure and better generalisation capability than the APF method. Further simulations were conducted for inspection robot path planning under normal working conditions, considering dynamic obstacles and an uncertain environment. The GBNN-based path-planning method can effectively solve path-planning problems for inspection robots encountering dynamic obstacles, avoiding congested sections, and performing emergency tasks during inspection processes.

Acknowledgement

This work was supported in part by the National Natural Science Foundation of China under Grant 52271321, 61873161, Shanghai Rising-Star Program under Grant 20QA1404200 and Natural Science Foundation of Shanghai under Grant 22ZR1426700.

References

[1] H. Liu, X. Huang, L. Tan, J. Guo, W. Wang, C. Yan, andC. Xu, Dynamic wireless charging for inspection robots based on decentralized energy pickup structure, *IEEE Transactions on Industrial Informatics*, *14*(4), 2018, 1786–1797.

[2] M. Cheng and D. Xiang, The design and application of a track-type autonomous inspection robotfor electrical distribution room, *Robotica*, *38*(2), 2020, 185–206.

[3] Q. Jiang, Y. Liu, Y. Yan, P. Xu, L. Pei, and X. Jiang, Active pose re localization for intelligent substation inspectionrobot, *IEEE Transactions on Industrial Electronics*, *70*(5), 2023, 4972–4982.

[4] U. Orozco-Rosas, O. Montiel, R. Sepúlveda, Mobile robot path planning using membrane evolutionary artificial potential field, *Applied Soft Computing*, *77*,2019, 236–251.

[5] Z. Pan, C. Zhang, Y. Xia, H. Xiong, and X. Shao, An improved artificial potential field method for path planning and formation control of the multi-UAV systems, *IEEE Transactions on Circuits and Systems II: Express Briefs*, *69*(3), 2021, 1129–1133.

[6] W. Pang, D. Zhu, and S. XYang, A novel time-varying formation obstacle avoidance algorithm for multi AUVs, *International Journal of Robotics and Automation*, 2023, DOI: https://doi.org/10.2316/J.2023.206-0845.

[7] B.K. Patle, L.G. Babu, A. Pandey, D.R.K. Parhi, and A. Jagadeesh, A review: On path planning strategies for navigation of mobile robot, *Defence Technology*, *15*(4), 2019, 582–606.

[8] X. Zhong, J. Tian, H. Hu, andX. Peng, Hybrid path planning based on safe Aalgorithm and adaptive window approach for mobile robot in large-scale dynamic environment, *Journal of Intelligent and Robotic Systems*, *99*, 2020, 65–77.

[9] H. Sang, Y. You, X. Sun, Y. Zhou, and F. Liu, The hybrid path planning algorithm based on improved A* and artificial potential field for unmanned surface vehicle formations, *Ocean Engineering*, *223*, 2021, 108709.

[10] F.H. Ajeil, I.K. Ibraheem, M.A. Sahib, and A.J. Humaidi, Multi-objective path planning of an autonomous mobile robot using hybrid PSO-MFB optimization algorithm, *Applied Soft Computing*, *89*, 2020, 106076.

[11] C. Luo, J. Gao, Y. L. Murphey, and G. E. Jan, A computationally efficient neural dynamics approach to trajectory planning of an intelligent vehicle, *IEEE International Joint Conference on Neural Network,* Beijing, China, 2014, 934–939.

[12] V.G. Nair and K.R. Guruprasad, Geodesic-VPC: Spatial partitioning for multi-robot coverage problem, *International Journal of Robotics and Automation*, 2020, *35*(3), 189–198.

[13] V.G. Nair and K.R. Guruprasad, GM-VPC: An algorithm for multi-robot coverage of known spaces using generalized Voronoi partition, *Robotica*, *38*(5), 2020, 845–860.

[14] V.G. Nair and K.R. Guruprasad, 2D-VPC: An efficient coverage algorithm for multiple autonomous vehicles, *International Journal of Control, Automation and Systems*, *19*(8), 2021, 2891–2901.

[15] C. Luo, S. X. Yang, X. Li, and M. Q.H. Meng, Neural-dynamics-driven complete area coverage navigation through cooperation of multiple mobile robots, *IEEE Transactions on Industrial Electronic*s, *64*(1), 2016, 750–760.

[16] B. Sun, D. Zhu, C. Tian, and C. Luo, Complete coverage autonomous underwater vehicles path planning based on glasius bio-inspired neural network algorithm for discrete and centralized programming, *IEEE transactions on cognitive and developmental systems*, *11*(1), 2018, 73–84.

[17] L. Han, X. Tan, Q. Wu, and X. Deng, An improved algorithm for complete coverage path planningbased on biologically inspired neural network, *IEEE Transactions on Cognitive and Developmental Systems*, 2023, DOI: https://doi.org/10.1109/TCDS.2023.3237612.

[18] D.V. Rodrigo, J.E. Sierra-Garc'ıa, andM. Santos, Glasius bio-inspired neural networks based UV-C disinfection path planning improved by preventive deadlock processing algorithm, *Advances in Engineering Software*, *175*, 2023, 103330.

[19] P. Yao and Z. Zhao, Improved Glasius bio-inspired neural network for target search by multiagents, *Information Sciences*, *568*, 2021, 40–53.

[20] P. Yao, K. Wu, and Y. Lou, Path Planning for Multiple Unmanned surface vehicles using glasius bio-inspired neural network with hungarian algorithm, *IEEE Systems Journal*, DOI: https://doi.org/10.1109/JSYST.2022.3222357.

[21] M.A.V.J. Muthugala, S.M.B.P. Samarakoon, and M.R. Elara, Toward energy-efficient online complete coverage path planning of a ship hull maintenance robot based on glasius bio-inspired neural network, *Expert Systems with Applications*, *187*, 2022, 115940.

[22] Z.L. Hu, J.H. Li, A. Chen, F. Xu, R. Jia, F.-L. Lin, and C.-B. Tang, Optimize grouping and path of pylon inspection in power system, *IEEE Access*, *8*, 2020, 108885–108895.

[23] N Chen andY. Wang, Design and collaborative operation of multimobile inspection robots in smart microgrids, *Complexity*, *2021*, 2021, 1–11.

[24] B. Wang, R. Guo, B. Li, L. Han, Y. Sun, and M. Wang, Smart Guard: An autonomous robotic system for inspecting substation equipment, *Journal of Field Robotics*, *29*(1), 2012, 123–137.

[25] B. Chen, H. Zhang, F. Zhang, Y. Liu, C. Tan, H. Yu, and Y. Wang, A multi-robot distributed collaborative region coverage search algorithm based on glasius bio-inspired neural network, *IEEETransactions on Cognitive and Developmental Systems*, 2022, DOI: https://doi.org/10.1109/TCDS.2022.3218718.

[26] D. Zhu, C. Tian, B. Sun, and C. Luo, Complete coverage path planning of autonomous underwater vehicle based on GBNN algorithm, *Journal of Intelligent and Robotic Systems*, *94*, 2019, 237–249.

Biographies

Wei Zhang was born in Xingtai, China. She received the M.S. degree in electrical engineering in 2013 and the Ph.D. degree in power electronics and power drives from Shanghai Maritime University in 2017. She is currently a Lecturer with Electrical Engineering and Automation, Shanghai Dianji University. Her research interests include motion control of substation inspection robot, formation control for multi-inspection robot systems, and power system control and optimization.

Xiaoliang Feng received the Ph.D. degree from Hohai University, China, in 2013. He is currently a Professor with the School of Electrical Engineering, Shanghai Dianji University, China. His current research interests include fault diagnosis, multi-source information fusion, and industrial data processing.

Bing Sun received the B.Sc. degree in communication engineering, the M.S. degree in communication and information systems, and the Ph.D. degree in power electronics and power transmission from Shanghai Maritime University, Shanghai, China, in 2009, 2011, and 2014, respectively. He is currently an Associate Professor with the Logistic Engineering Colleague, Shanghai Maritime University. His current research interest includes motion planning and tracking control of underwater vehicles and multi-AUV systems.